Original Article

Upregulation of TMCO3 Promoting Tumor Progression and Contributing to the Poor Prognosis of Hepatocellular Carcinoma

Tianxing Dai[1,2], Linsen Ye[1,2], Mingbin Deng[1,2], Guozhen Lin[2,3], Rongqiang Liu[2,4], Haoyuan Yu[1,2], Wei Liu[2], Yang Yang[1] and Guoying Wang[4]*

[1]Department of Hepatic Surgery and Liver Transplant Program, The Third Affiliated Hospital of Sun Yat-Sen University, Guangzhou, Guangdong, China; [2]Guangdong Key Laboratory of Liver Disease Research, The Third Affiliated Hospital of Sun Yat-Sen University, Guangzhou, Guangdong, China; [3]Department of Hepatic Surgery, The Third People's Hospital of Shenzhen, Shenzhen, Guangdong, China; [4]Department of Hepatobiliary Surgery, The First Affiliated Hospital of Guangzhou Medical University, Guangzhou, Guangdong, China

Abstract

Background and Aims: TMCO3, a member of the monovalent cation:proton antiporter-2 family, has been annotated as a Na^+/H^+ antiporter, but its pathophysiological role is still unclear. We aimed to investigate the expression profile, prognostic significance, and oncogenic role of TMCO3 in hepatocellular carcinoma (HCC). ***Methods:*** Bioinformatic analyses were conducted using transcriptome data from public databases to determine the expression, prognosis, and functional enrichment of TMCO3 in HCC. TMCO3 expression was further validated in an independent HCC cohort from our institution. The oncogenic role of TMCO3 in HCC was evaluated using *in vitro* and *in vivo* experiments. ***Results:*** The upregulated expression of TMCO3 was identified and verified in multiple HCC cohorts, and worse overall survival and recurrence-free survival were observed in patients with high TMCO3 expression. The overexpression and knockdown of TMCO3 could affect the proliferation and metastasis of HCC cells, which might be associated with the p53-induced cell cycle regulation and epithelial-mesenchymal transition, respectively. Notably, significant correlations were found between dysregulated TMCO3 and various antitumor agents. Its role in sorafenib sensitivity was further identified by *in vitro* experiments and the potential mechanism might be related to the regulation of apoptosis. Positive correlations were also identified between upregulation of TMCO3 and the increased infiltration of various immune cells and the elevated expression of multiple immune checkpoint genes in HCC. ***Conclusions:*** Upregulated TMCO3 could act as an oncogenic mediator and promote sorafenib resistance in HCC, providing a potential therapeutic target for HCC treatment.

Introduction

The global morbidity of liver cancer remains high, with more than 800,000 new cases reported annually, and is the fourth leading cause of cancer-related death.[1] Hepatocellular carcinoma (HCC), as the major pathological type, accounts for almost 90% of all cases. Chronic hepatitis caused by viral infection (such as hepatitis B and C viruses) and cirrhosis are important causes of HCC. Curative treatment strategies, including surgical resection and liver transplantation, can only be provided to a limited proportion of HCC patients in the early stage of the disease.[2] The advent of sorafenib, the first approved targeted therapy, provides a new opportunity for the treatment of advanced HCC.[3] However, the relatively low proportion of the population who are responsive to this medication and the high rate of drug resistance limit its efficiency. Recently, immunotherapy with immune checkpoint inhibitors (ICIs) has opened a new era for treating advanced HCC, but there are also concerns about efficiency.[4,5] Hence, further investigation of the pathogenesis of HCC will help determine new therapeutic targets and improve the

existing treatments.

TMCO3, also known as transmembrane and coiled-coil domains 3 or C13orf11, is a protein-coding gene with functional annotation of probable Na^+/H^+ antiporter. It belongs to the monovalent cation:proton antiporter-2 (CPA2) family according to the Transporter Classification Database (TCDB).[6] Most CPA2 family members have similar functions and are involved in ion transport (K^+, Na^+, and H^+) in bacteria, archaea, insects, and plants. However, investigations on the function of TMCO3 are insufficient. Recently, Chen *et al*.[7] found that TMCO3 is expressed in the human cornea, lens capsule, and choroid-RPE, and that TMCO3 mutations were associated with the development of cornea guttata and anterior polar cataract in the Chinese population. Besides, the TMCO3 mutation in plasma cell-free DNA was also identified in neuroblastoma patients undergoing chemotherapy, and was positively correlated with bone marrow genomic DNA.[8] Another study conducted in patients with dystonia found that TMCO3 was sequenced in a chromosome 13q34 duplication, but its significance was not elucidated.[9] These findings provide clues to the pathophysiological role of TMCO3, but further research is needed.

To our knowledge, our study presented herein is the first to determine the expression characteristics and potential role of TMCO3 in HCC. First, we evaluated the expression profile, regulation network, functional enrichment, and correlation with drug susceptibility and tumor immune microenvironment of TMCO3 using bioinformatics analyses. *In vitro* and *in vivo* experiments were conducted to validate its expression and explore its function and underlying mechanisms in HCC. Notably, its role in regulating sorafenib sensitivity was also explored, which may provide a new potential target for the treatment of HCC.

Methods

Patients and specimens

A total of 105 newly diagnosed HCC patients who underwent curative resection at The Third Affiliated Hospital of Sun Yat-Sen University from January 2018 to December 2019 were enrolled in this study. Tumor and adjacent normal tissue samples (stored at −80°C) from 52 patients were collected for protein and RNA extraction, while paraffin-embedded tissue samples were collected from all study patients for histological analysis. Written informed consent was obtained from all the enrolled patients. The study was approved by the Ethics Committee of The Third Affiliated Hospital of Sun Yat-Sen University and in accordance with the standards of the Declaration of Helsinki.

Cell lines and culture

Human hepatoma cell lines Huh7, MHCC97-H, LM3, and Hep-G2, and the normal liver cell line L02 were obtained from the Shanghai Cell Bank of the Chinese Academy of Sciences. The cells were cultured in Dulbecco's modified Eagle's medium (Gibco, Carlsbad, CA, USA) supplemented with 1% penicillin/streptomycin (Gibco) and 10% fetal bovine serum (FBS; PAN-Biotech, Aidenbach, Germany) in a humidified incubator at 37°C and with 5% CO_2.

Gene silencing and overexpression by lentiviral vectors

Stable HCC cells (Huh7 and LM3) silenced for TMCO3 ex-

pression were constructed using lentiviral vehicles expressing short hairpin (sh)TMCO3 (sh-1 and sh-2) and negative control (sh-NC), and stable TMCO3 overexpressing Hep-G2 cells were also transfected with lentiviral vectors, which were all designed and purchased from GenePharma Co. Ltd (Shanghai, China). Lentivirus transduction was performed using polybrene. Cell lines with TMCO3 overexpression and knockdown were selected and enriched in the medium with puromycin.

RNA extraction and quantitative reverse transcription-polymerase chain reaction

Total RNA from cultured cells and tissues was extracted using TRIzol reagent (Invitrogen, Carlsbad, CA, USA). cDNA was synthesized using the Transcriptor First-Strand cDNA Synthesis Kit (Roche, Basel, Switzerland) with 2 µg RNA. Then, quantitative reverse transcription-polymerase chain reaction (qRT-PCR) was conducted using the SYBR Green I PCR Master Mix (Roche) with a LightCycler 480 Real-Time PCR System (Roche). All procedures were performed according to the manufacturer's instructions. Glyceraldehyde 3-phosphate dehydrogenase (GAPDH) was used as an internal control. The relative expression levels were calculated using the 2-ΔΔCt method. All primers were designed and synthesized by Sangon Biotech (Shanghai, China). The primer sequences were as follows: TMCO3, 5'-CCAGAAGAATGCAGTTCTGAAC-3' (forward) and 5'-CTGGAAAATTTCAAACGTGTGC-3' (reverse) and GAPDH, 5'-TGCACCACCAACTGCTTAGC-3' (forward) and 5'-GGCATGGACTGTGGTCATGAG-3' (reverse).

Cell Counting Kit-8 assay

The transfected HCC cells (Huh7, LM3, and Hep-G2) were seeded in 96-well plates (1,000 cells/well). Cell proliferation was measured every 24 h for 5 days using the Cell Counting Kit-8 (CCK-8) reagent (APExBIO, Houston, TX, USA). After incubation with 10 µL of CCK-8 solution mixed with 90 µL fresh medium at 37°C for 2 h, the optical density value at 450 nm was measured using a spectrophotometer.

Colony formation assay

The transfected HCC cells were plated in 6-well plates (1,000 cells/well) and incubated for 14 days. The colonies were then fixed with 4% paraformaldehyde (PFA) and stained with 0.1% crystal violet at room temperature. The colonies formed with more than 50 cells were counted using ImageJ software.

5-Ethynyl-2'-deoxyuridine assay

The 5-Ethynyl-2'-deoxyuridine (EDU) Cell Proliferation Kit with Alexa Fluor 594 (Beyotime, Shanghai, China) was used according to the manufacturer's instructions. The transfected cells were incubated with 10 µM EDU for 2 h and stained with DAPI. Images were acquired using an inverted fluorescence microscope (Carl Zeiss, Jena, Germany). Cell proliferation was evaluated based on the proportion of EDU-positive cells.

Flow cytometry for cell cycle analysis

The transfected cells were collected and fixed with 70%

ethanol overnight at 4°C. Then, the fixed cells were resuspended in phosphate-buffered saline containing ribonuclease A and stained with propidium iodide for 30 m in the dark at room temperature. The proportions of cells in different phases of the cell cycle were analyzed using a FACS Calibur flow cytometer (BD Biosciences, San Jose, CA, USA).

Wound healing assay

The transfected cells were seeded in 6-well plates (5×10^5 cells/well) and maintained for 24 h at 37°C. When the cells were fully confluent, the wound was created using a sterile 10-µL pipet tip. The scratched area was recorded with five random fields at 0 and 48 h, and then calculated using ImageJ software.

Transwell invasion assay

The HCC cells resuspended in FBS-free medium were seeded in the upper chamber separated by transwell inserts (Millipore, Burlington, MA, USA), which was coated with 10% Matrigel (BD Biosciences, San Jose, CA). The lower chamber was supplemented with 500 µL medium containing 20% FBS. After incubation for 36 h, the Transwell inserts were fixed with 4% PFA and stained with 0.1% crystal violet. Afterward, the cells in the upper chamber were wiped off, while the cells retained on the back side were invaded cells, which were further recorded and quantified with five random fields under an inverted microscope.

Western blot

The total proteins of cultured cells and tissues were extracted using a radioimmunoprecipitation assay lysis buffer and separated by sodium dodecyl sulfate-polyacrylamide gel electrophoresis. The proteins were then transferred to a polyvinylidene difluoride membrane and blocked with 5% non-fat milk powder for 1 h at room temperature. The membrane was further incubated with diluted primary antibodies at 4°C overnight and the corresponding secondary antibodies at room temperature for 1 h. The protein signals were detected using an enhanced chemiluminescence detection system. GAPDH was used as an internal control. The primary antibody for detecting TMCO3 (1:2,000) was purchased from Abcam (Cambridge, MA, USA). The antibodies for detection of GAPDH (#5174, 1:2,000), p53 (#2527, 1:1,000), p21 (#2947, 1:1,000), ZO1 (#8193, 1:1,000), E-cadherin (#3195, 1:1,000), Puma (#12450, 1:1,000), Bim (#2933, 1:1,000), PARP (#9542, 1:1,000), Caspase 3 (#14220, 1:1,000), p38 MAPK (#8690, 1:1,000), and phospho-p38 MAPK (Thr180/Try182) (#4511, 1:1,000) were purchased from Cell Signaling Technology (Danvers, MA, USA). The experiments were independently performed in triplicate.

Histology and immunohistochemistry

All tissue samples were fixed in 4% PFA, embedded in paraffin, and sectioned (4 µm thickness). Hematoxylin and eosin staining was performed using standard methods. For immunohistochemistry (IHC), after dewaxing and dehydration, the tissue sections were treated with ethylenediaminetetraacetic acid buffer (pH 8.0) for antigen retrieval. The cells were then incubated with 3% H_2O_2 and blocked with 10% goat serum. The sections were incubated with primary antibodies overnight at 4°C and the respective secondary

antibodies for 1 h at 37°C. Diaminobenzidine was used for chromogenic reaction, and hematoxylin was used for counterstaining.

Animal studies

Six-week-old BALB/c nude mice were purchased from the Guangdong Medical Laboratory Animal Center (Guangdong, China) and bred in-house in specific pathogen-free environments. The animal care program was implemented in accordance with the guidelines of the Sun Yat-Sen University for Animal Experimentation. A total of 5×10^6 transfected HCC cells were subcutaneously implanted in the backs of mice (*n*=5 per group). The tumor volume was monitored and calculated as (length×width^2)/2 weekly. Four weeks later, the mice were euthanized, and the tumors were collected, photographed, and weighed. All procedures were approved by the Institutional Animal Care and Use Committee of the Third Affiliated Hospital of Sun Yat-Sen University.

Bioinformatics analysis

Datasets: The transcriptome data of HCC were obtained from The Cancer Genome Atlas (TCGA) (https://portal.gdc.cancer.gov/) and Gene Expression Omnibus (GEO) (https://www.ncbi.nlm.nih.gov/geo/). In the TCGA-LIHC cohort, 374 HCC tumor samples and 50 normal controls were used for gene expression analyses, while only 370 cases with valid clinical information were used for survival analyses. The expression of TMCO3 was further validated using data from GSE14520 (T: 225/N: 220), GSE25097 (T: 268/N: 243), GSE76297 (T: 62/N: 59), and GSE39791 (T: 72/N: 72). The expression profiles of TMCO3 in other types of gastrointestinal cancers (cholangiocarcinoma [CHOL], colon adenocarcinoma [COAD], esophageal carcinoma [ESCA], pancreatic adenocarcinoma [PAAD], rectum adenocarcinoma [READ], and stomach adenocarcinoma [STAD]) were analyzed using Gene Expression Profiling Interactive Analysis (http://gepia.cancer-pku.cn).[10]

Protein-protein interaction and functional enrichment analyses: The protein-protein interaction (PPI) networks of TMCO3 were analyzed using the Search Tool for Retrieval of Interacting Genes/Proteins (STRING, version 11; https://string-db.org/) and GeneMANIA (http://genemania.org/).[11,12] The coexpressed genes with TMCO3 in HCC were identified by correlation analyses (correlation coefficient >0.5, and *p*<0.01). Functional enrichment analyses, including Gene Ontology (GO) and Kyoto Encyclopedia of Genes and Genomes (KEGG), were performed based on the coexpression network of TMCO3 in HCC.

Correlation analyses with DNA methylation, drug susceptibility, and immune microenvironment: The DNA methylation data with the platform of Illumina Human Methylation 450 for TCGA HCC patients were downloaded from UCSC Xena (https://xenabrowser.net/). The CpG sites in the promoter regions of TMCO3 and the corresponding methylation levels were extracted. The correlation between gene expression and methylation was determined using Pearson's correlation analysis. The drug susceptibility analyses were conducted using the R package "pRRophetic" with data from the Genomics of Drug Sensitivity in Cancer (GDSC) database to compare the half-maximum inhibitory concentration, the IC50, of the samples between low- and high-expression groups of TMCO3 (median as the cutoff value).[13] The correlations of TMCO3 expression with infiltration levels of various immune cells and immune checkpoint genes in HCC were analyzed on TIMER (https://cistrome.shinyapps.io/timer/).[14]

Statistical analysis

All statistical analyses were performed using GraphPad Prism 5.0 (GraphPad Software, San Diego, CA, USA) and R 4.0.3 software (https://www.r-project.org/). Data are presented as mean±standard deviation derived from three independent experiments. One-way analysis of variance was used for multiple-group comparisons, while Student's *t*-test was used for comparison of two unpaired groups. Correlation analysis was conducted using the Pearson's *r* test. The survival curves were plotted using the Kaplan-Meier method and analyzed using the log-rank test. The overall survival (OS) from the TCGA cohort was defined as the interval between the date of treatment and either the date of death or last follow-up, and the survival information was obtained from the public database in December 2020. Recurrence-free survival (RFS) was defined as the interval between the date of surgery and the date of confirmed recurrence. If recurrence had not occurred within the follow-up period (to December 31, 2020), the cases were censored on the date of death or the last date of follow-up. Statistical significance was set at $p<0.05$.

Results

Expression profile and prognostic significance of TMCO3 in HCC

The expression profile of TMCO3 in HCC was initially evaluated using transcriptome data from the TCGA-LIHC dataset. The differential analysis of all samples (T: 374/N: 50) indicated that the mean expression level of TMCO3 in HCC tumors was significantly higher than that in normal controls ($p<0.001$; Fig. 1A). A comparison between 50 paired tumor and para-tumor samples also showed that the TMCO3 expression was significantly upregulated in HCC tumors ($p<0.001$; Fig. 1B). Analyses of clinicopathological factors suggested that higher expression of TMCO3 was found in tumors with advanced pathological grades ($p=0.007$; Fig. 1C). The worse OS rate was also identified in HCC patients with higher TMCO3 expression by survival analysis ($p<0.0001$; Fig. 1D). The clinicopathological characteristics of the high and low TMCO3 expression groups are summarized in Supplementary Table 1.

The elevated expression characteristics of TMCO3 in HCC were further validated in other independent datasets: GSE14520 ($p<0.001$; Fig. 1E), GSE25097 ($p<0.001$; Fig. 1F), GSE76297 ($p<0.001$; Fig. 1G), and GSE39791 ($p<0.001$; Fig. 1H). Furthermore, we evaluated the TMCO3 expression in other types of gastrointestinal cancers; the results indicated that, except for HCC, TMCO3 was significantly upregulated in CHOL ($p<0.01$), whereas no significant difference was found in COAD, ESCA, PAAD, READ, and STAD (all $p>0.05$) (Fig. 1I).

Functional enrichment analyses

The PPI network analyses of TMCO3 using STRING (Fig. 2A) and GeneMANIA (Fig. 2B) prediction tools indicated that the SLC9A/B/C members (such as SLC9A9, SLC9B1, and SLC9C1) might have extensive interactions with TMCO3. These SLC9 family members are mostly involved in the regulation of the transmembrane exchange of Na^+ and H^+, which is similar to the functional annotation of TMCO3. In addition, other proteins with potential interactions with TMCO3, such as LAMTOR1, TRMT2A, MED16, and CGR, were also identified, which indicated its likely functions in

other aspects. The coexpression network of TMCO3 in HCC was established based on the gene expression correlation analyses. A total of 1,592 genes (positive: 1,571/negative: 21) were identified with a coefficient of >0.5 and a *p* value of <0.01. The top 25 genes with positive and negative correlations with TMCO3 were shown in a heatmap (Fig. 2C), while the five most significantly correlated genes (positive: UGGT2, ATP11A, RAP2A, STK24, and NSD2; negative: DCXR, SLC27A5, GLYAT, ASPDH, and ADI1) were shown in expression correlation plots (Fig. 2D).

Based on the coexpression network, results from GO analyses indicated that TMCO3 might participate in the chromosome segregation, cell cycle checkpoint, and histone modification (biological process), ATPase activity, transcription coactivator activity, and histone acetyltransferase activity (molecular function) (Fig. 2E). The results of KEGG further suggested that TMCO3 might be involved in the regulation of cell cycle, spliceosome, cellular senescence, and ubiquitin mediated proteolysis (Fig. 2F). Therefore, the regulation of cell cycle might be crucial for TMCO3 to play a role in HCC.

Correlation analyses between TMCO3 and DNA methylation, drug susceptibility, and tumor immune microenvironment

As one of the most common regulatory mechanisms of gene expression, the DNA methylation profile of TMCO3 was also evaluated using the TCGA dataset. A total of 20 methylation CPG sites in the promoter of TMCO3 were recognized with their corresponding methylation levels (beta values) (Fig. 3A). Then, the correlation between the methylation level of each CPG site and the expression level of TMCO3 was analyzed. Results indicated that the methylation of CPG sites with cg09715768 ($R=-0.21, p=6.6e-05$), cg21152981 ($R=-0.31, p=7.9e-10$), cg11357670 ($R=-0.32, p=5e-10$), cg27560367 ($R=-0.33, p=5.7e-11$), and cg24164238 ($R=-0.32, p=4.9e-10$) was negatively correlated with TMCO3 expression, whereas the methylation of CPG sites with cg13412514 ($R=0.23, p=5.5e-06$) and cg24121069 ($R=0.22, p=1.5e-05$) was positively correlated with TMCO3 expression (Fig. 3B). The overall methylation level of TMCO3 was negatively correlated with its gene expression ($R=-0.34, p=2.1e-11$; Fig. 3B).

To explore the potential influence of dysregulated TMCO3 on HCC treatment, we evaluated the correlation between the sensitivity of HCC cells to chemotherapeutic drugs and TMCO3 expression. Results showed that higher TMCO3 expression was correlated with higher IC50 values of cisplatin, metformin, rapamycin, sunitinib, and sorafenib (all $p<0.05$; Fig. 3C), which indicated less sensitivity or a higher probability of resistance. However, the lower IC50 values of doxorubicin, etoposide, gemcitabine, mitomycin C, and lapatinib were also observed in HCC patients with higher expression of TMCO3 (Fig. 3C). These findings may serve as a reference for the precise treatment of HCC.

We also evaluated the role of elevated TMCO3 levels in the tumor immune microenvironment of HCC. Based on the estimated results from the TIMER, positive correlations were found between the upregulation of TMCO3 and the high infiltration levels of B cells ($R=0.315, p=2.26e-09$), CD8+ T cells ($R=0.212, p=7.93e-05$), CD4+ T cells ($R=0.428, p=8.87e-17$), macrophages ($R=0.435, p=3.60e-17$), neutrophils ($R=0.402, p=7.55e-15$), and dendritic cells ($R=0.375, p=8.55e-13$) (Fig. 3D). Positive correlations between TMCO3 expression and immune checkpoint gene expression were also identified in programmed death 1 (PD-1) ($R=0.233, p=5.81e-06$), programmed death-ligand 1 (PD-L1) ($R=0.293, p=8.98e-09$), cytotoxic T lymphocyte antigen-4 (CTLA4)
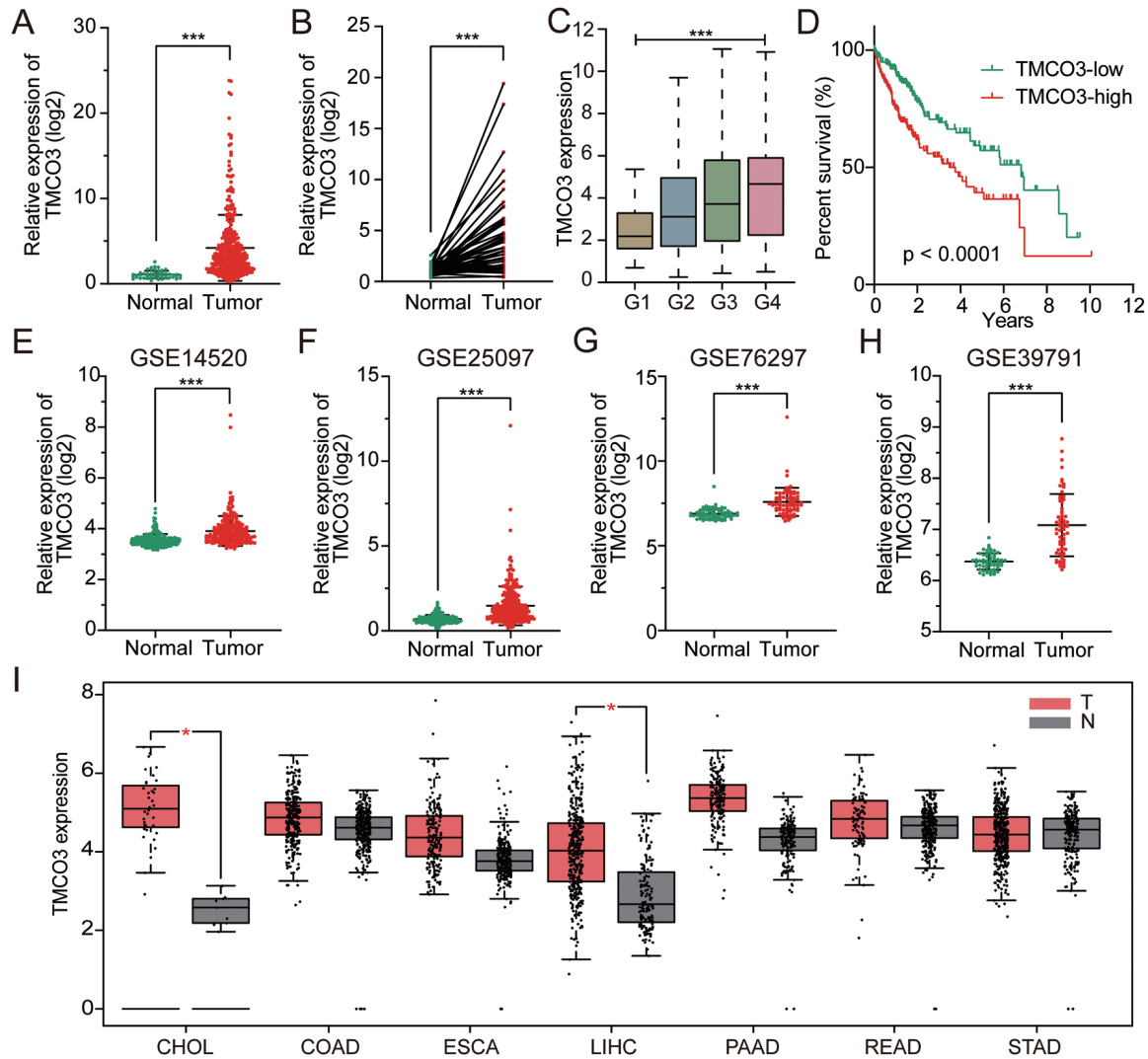
Fig. 1. Expression profile and prognostic significance of TMCO3 in HCC. (A) TMCO3 is upregulated in HCC tumors compared to NCs in the TCGA cohort (tumor: n=374/normal: n=50). (B) Relative expression of TMCO3 in 50 paired HCC tumors and NCs in the TCGA cohort. (C) Differential expression of TMCO3 in different pathological grades of HCC. (D) Patients with high expression of TMCO3 had worse overall survival in the TCGA cohort. (E–H) Validation of the TMCO3 expression profile in HCC with GSE14520 (tumor: n=225/normal: n=220), GSE25097 (tumor: n=268/normal: n=243), GSE76297 (tumor: n=62/normal: n=59), and GSE39791 (tumor: n=72/normal: n=72) cohorts. (I) Expression profile of TMCO3 in different gastrointestinal cancers by Gene Expression Profiling Interactive Analysis (http://gepia. cancer-pku.cn). *p<0.05; ***p<0.001. CHOL, Cholangio carcinoma; COAD, Colon adenocarcinoma; ESCA, Esophageal carcinoma; PAAD, Pancreatic adenocarcinoma; READ, Rectum adenocarcinoma; STAD, Stomach adenocarcinoma; HCC, hepatocellular carcinoma; NC, normal control; TCGA, The Cancer Genome Atlas.

(R=0.177, p=6.3e−04), TIM3 (R=0.325, p=1.91e−10), T cell immunoreceptor with Ig and ITIM domains (TIGIT) (R=0.235, p=4.75e−06), and B7-H3 (CD276; R=0.518, p<0.0001) (Fig. 3E). These results indicate the potential role of TMCO3 in the regulation of the immunosuppressive microenvironment of HCC.

Expression validation of TMCO3 in our independent cohort of HCC patients

To further validate the expression profile of TMCO3 in HCC, an independent cohort from our institution was recruited for this study. The correlations between TMCO3 expression and the clinicopathological factors are summarized in Supplementary Table 2. First, qRT-PCR was conducted to evaluate the TMCO3 mRNA levels in 52 paired HCC tumors and ad-

jacent normal tissues. Results showed that TMCO3 was upregulated in most HCC tumors (n=31, 59.6%; Fig. 4A), and its mean expression in tumors was also significantly higher than that in adjacent tissues (p<0.01; Fig. 4B). Survival analysis further confirmed that patients with high TMCO3 expression had lower RFS rates (p=0.0305; Fig. 4C). The protein expression profile of TMCO3 in HCC was determined using immunoblotting and IHC. Western blotting results from eight cases showed that the TMCO3 protein was upregulated in most HCC tumors (n=5, 62.5%; Fig. 4D). The IHC results from 105 paired paraffin-embedded tissue sections showed moderate to high expression levels of TMCO3 in most HCC tumors, while the majority of adjacent tissues showed low expression levels of TMCO3 (Fig. 4E). A higher mean protein expression level of TMCO3 was further identified in HCC tumors based on the immunohistochemical score (Fig. 4E).
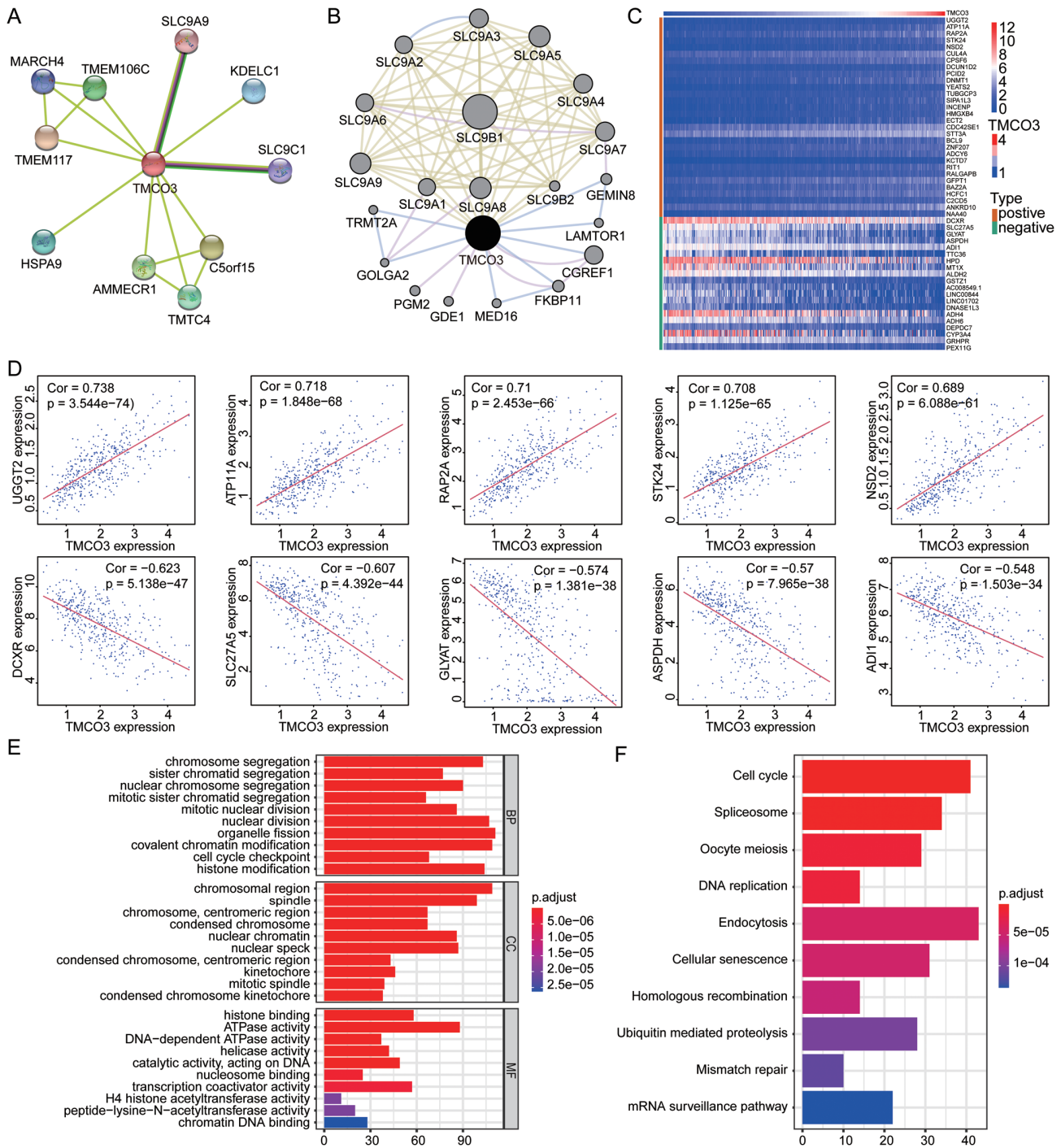
Fig. 2. Functional analyses of TMCO3. (A and B) PPI networks of TMCO3 established by the STRING and GeneMANIA online tools. (C) Heatmap of the top 50 co-expressed genes with positive and negative correlation with TMCO3 in HCC. (D) Expression correlation plots of the top 10 coexpressed genes with TMCO3. (E and F) GO and KEGG analyses for the functional estimation of TMCO3 in HCC. GO, Gene Ontology; HCC, hepatocellular carcinoma; KEGG, Kyoto Encyclopedia of Genes and Genomes; PPI, protein-protein interaction.

Dysregulated TMCO3 is involved in regulating cell proliferation by affecting the cell cycle transformation

To characterize the oncogenic mechanism of TMCO3, its role in cell proliferation was further explored. TMCO3 gene and protein expression were upregulated more in a variety of hepatoma cell lines (Hep-G2, Huh7, LM3, and MHCC-97H) than in normal hepatocytes (L02) (Supplementary Fig. 1A–B). Two HCC cell lines (Huh7 and LM3) with relatively high expression of TMCO3 were selected to construct sta-
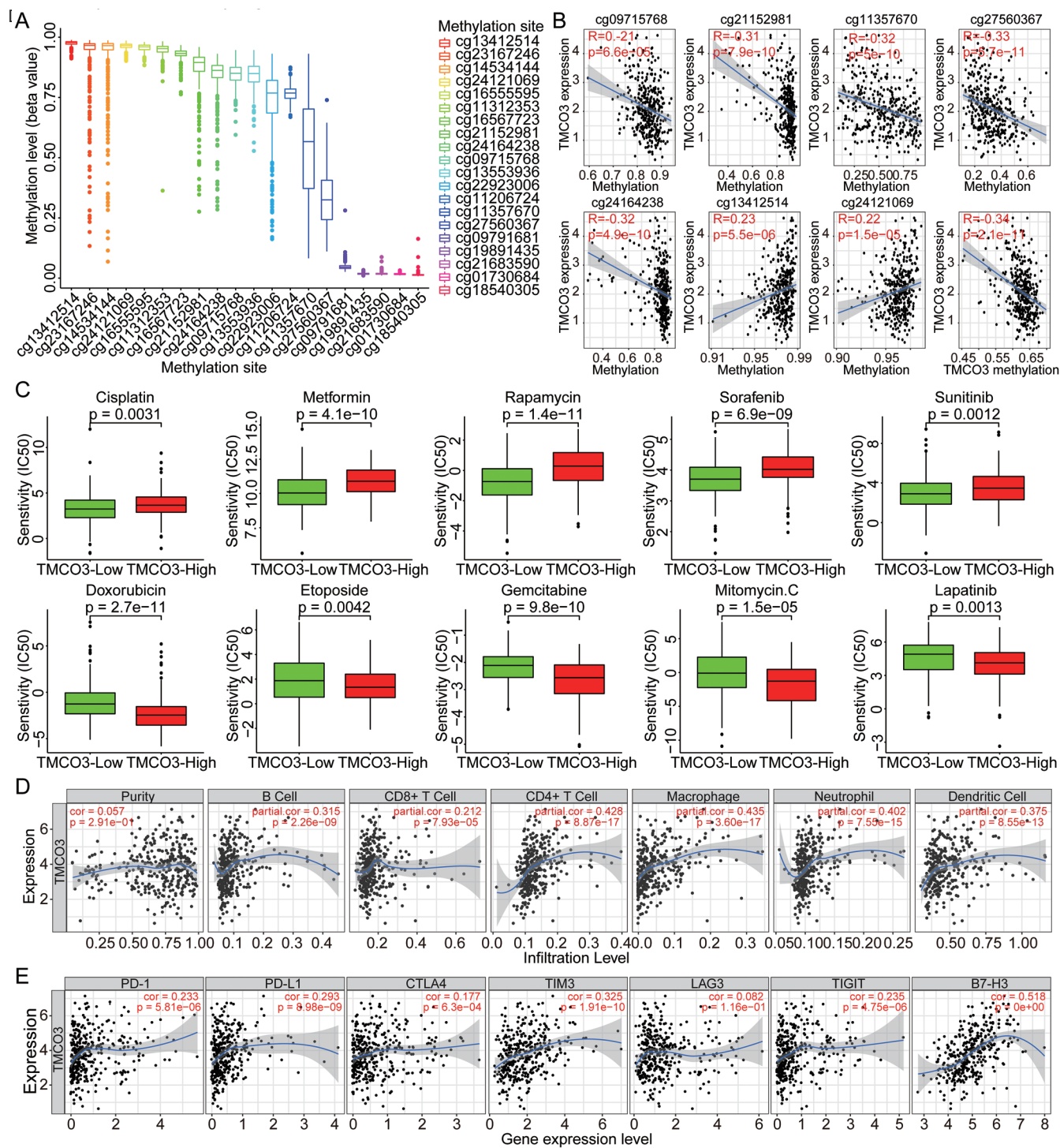
Fig. 3. Correlation analyses between TMCO3 expression and DNA methylation, drug susceptibility, and tumor immune microenvironment of HCC. (A) Methylation levels of different CPG sites in TMCO3 promoter. (B) Correlations between TMCO3 gene expression and specific methylation levels. (C) Susceptibility analyses with IC50 of different agents in groups with high- and low-expression of TMCO3. (D and E) Correlation analyses between TMCO3 expression levels and the infiltration levels of various immune cells and the expression levels of immune checkpoint genes in HCC. HCC, hepatocellular carcinoma; IC50, half maximal inhibitory concentration.

bly transfected cell models with TMCO3 suppression; the knockdown efficiency at the gene and protein levels are shown in Supplementary Figure 1C–D. The Hep-G2 cell line with relatively low expression levels was selected for the treatment of TMCO3 overexpression (Supplementary Fig. 1E–F). The cell viability assay with CCK-8 showed that both

Huh7 and LM3 cells with TMCO3 knockdown had a slower growth rate compared with the control cells, whereas the Hep-G2 overexpressing TMCO3 showed an enhanced proliferation rate (all *p*<0.05; Fig. 5A). The number of colonies was also markedly decreased in the Huh7 and LM3 cells with TMCO3 knockdown, whereas it increased in the TM-
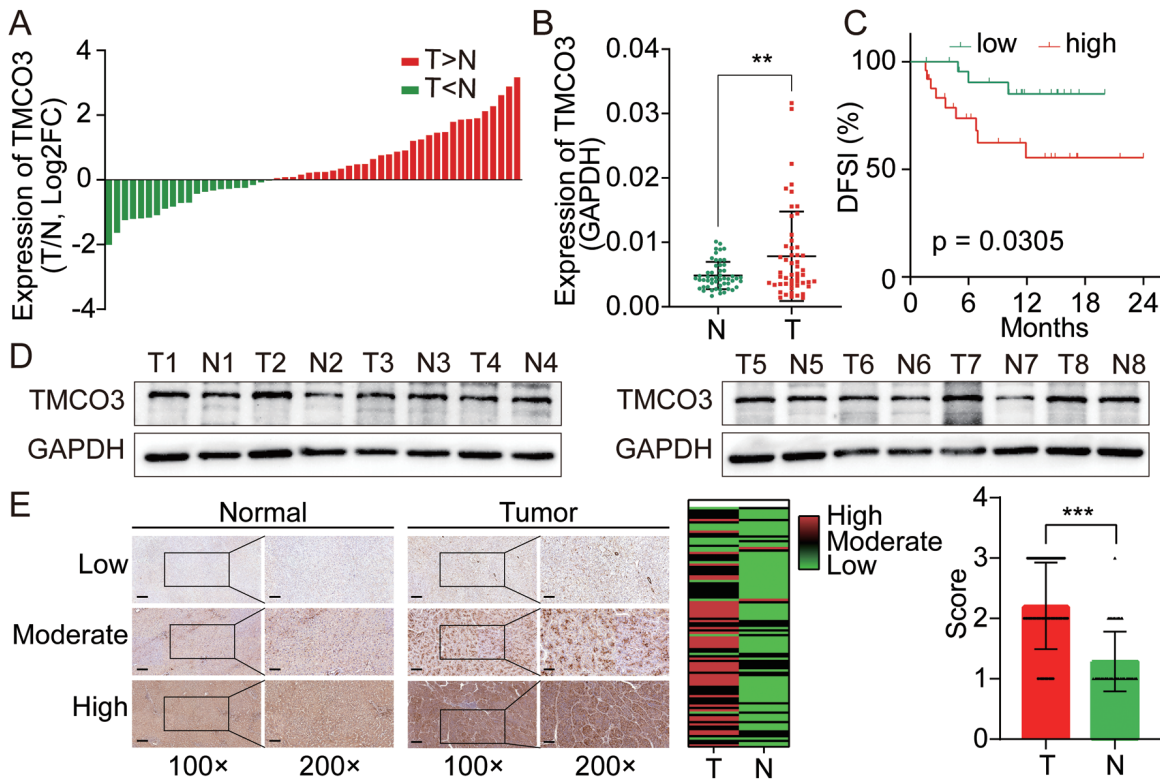
Fig. 4. Validation of TMCO3 expression in the HCC cohort from our institution. (A) Relative RNA expression of TMCO3 in HCC tumors compared with NCs (*n*=52). (B) Higher mean expression level of TMCO3 in HCC tumors (tumor: *n*=52/normal: *n*=52). (C) HCC patients with high TMCO3 expression had worse RFS. (D) TMCO3 protein expression tested by western blot in paired tissue samples from eight HCC patients. (E) Representative IHC images of TMCO3 in HCC tumors and NCs (left panel), IHC expression intensity (heatmap, middle panel) and scores (right panel) of 105 paired HCC tumors and normal tissue samples (scale bar, 50 μm). **$p<0.01$; ***$p<0.001$. HCC, hepatocellular carcinoma; IHC, immunohistochemistry; NC, normal control; RFS, recurrence-free survival.

CO3-overexpressing Hep-G2 cells (all $p<0.001$; Fig. 5B). In addition, when the TMCO3 was suppressed, the proportion of EDU-positive cells decreased in both transfected HCC cell lines; meanwhile, an opposite result was observed in the TMCO3-overexpressing Hep-G2 cells (all $p<0.001$; Fig. 5C). Based on these *in vitro* findings and the prediction results from functional enrichment analyses, we investigated the role of TMCO3 in the regulation of cell cycle progression in HCC cells. Results showed that knockdown of TMCO3 significantly increased the proportion of Huh7 and LM3 cells in the G1 phase, but decreased the proportion of cells in the G2 phase compared with controls (Fig. 5D). In the TM-CO3-overexpressing Hep-G2 cells, the proportion of cells decreased in the G1 phase (Fig. 5D). As expected, western blot analysis showed that the protein expression of negative cell cycle regulators p53 and p21 was increased in Huh7 and LM3 cells with TMCO3 knockdown, as well as the phosphorylation of p38 MAPK (Thr180/Tyr182) (Fig. 5E). The expression of p53 and p21 proteins and phosphorylation of p38 MAPK were reduced in TMCO3-overexpressing Hep-G2 cells (Fig. 5E). These results indicated the potential mechanism by regulating the p53-induced cell cycle to affect the HCC proliferation.

Dysregulated TMCO3 regulating the migration and invasion abilities of HCC cells

The role of TMCO3 in the metastasis of HCC cells was further investigated using *in vitro* metastasis assays. The results of scratch wound healing assays showed that

knockdown of TMCO3 significantly inhibited the migratory capacity of Huh-7 and LM3 cells, whereas the overexpression of TMCO3 in Hep-G2 cells enhanced their migration ability (all $p<0.001$; Fig. 6A). The transwell Matrigel invasion assay also showed that knockdown of TMCO3 significantly suppressed the invasion of Huh-7 and LM3 cells, while the overexpression of TMCO3 enhanced the invasion ability of Hep-G2 cells (all $p<0.001$; Fig. 6B). Subsequently, the epithelial-mesenchymal transition (EMT)-related proteins, which are closely related to the metastasis of tumors, were evaluated by western blot analysis. Results indicated that the protein expression of epithelial phenotype markers with ZO-1 and E-cadherin was significantly upregulated in HCC cells with TMCO3 knockdown and decreased in TMCO3-overexpressing cells (Fig. 6C). These results indicated that TMCO3 suppression might inhibit the *in vitro* migration and invasion of HCC cells by regulating the EMT process.

Dysregulated TMCO3 modulating the sensitivity of HCC cells to sorafenib

Bioinformatic analyses revealed a significant correlation between TMCO3 expression and the sensitivity of HCC cells to sorafenib. Hence, we further explored the effect of TMCO3 on the antitumor effects of sorafenib. Results showed that the IC50 of sorafenib was markedly decreased in Huh7 and LM3 cells with TMCO3 suppression (all $p<0.01$; Fig. 7A). In Hep-G2 cells, the IC50 of sorafenib increased with TMCO3 overexpression ($p<0.01$; Fig. 7A). Western blotting analysis
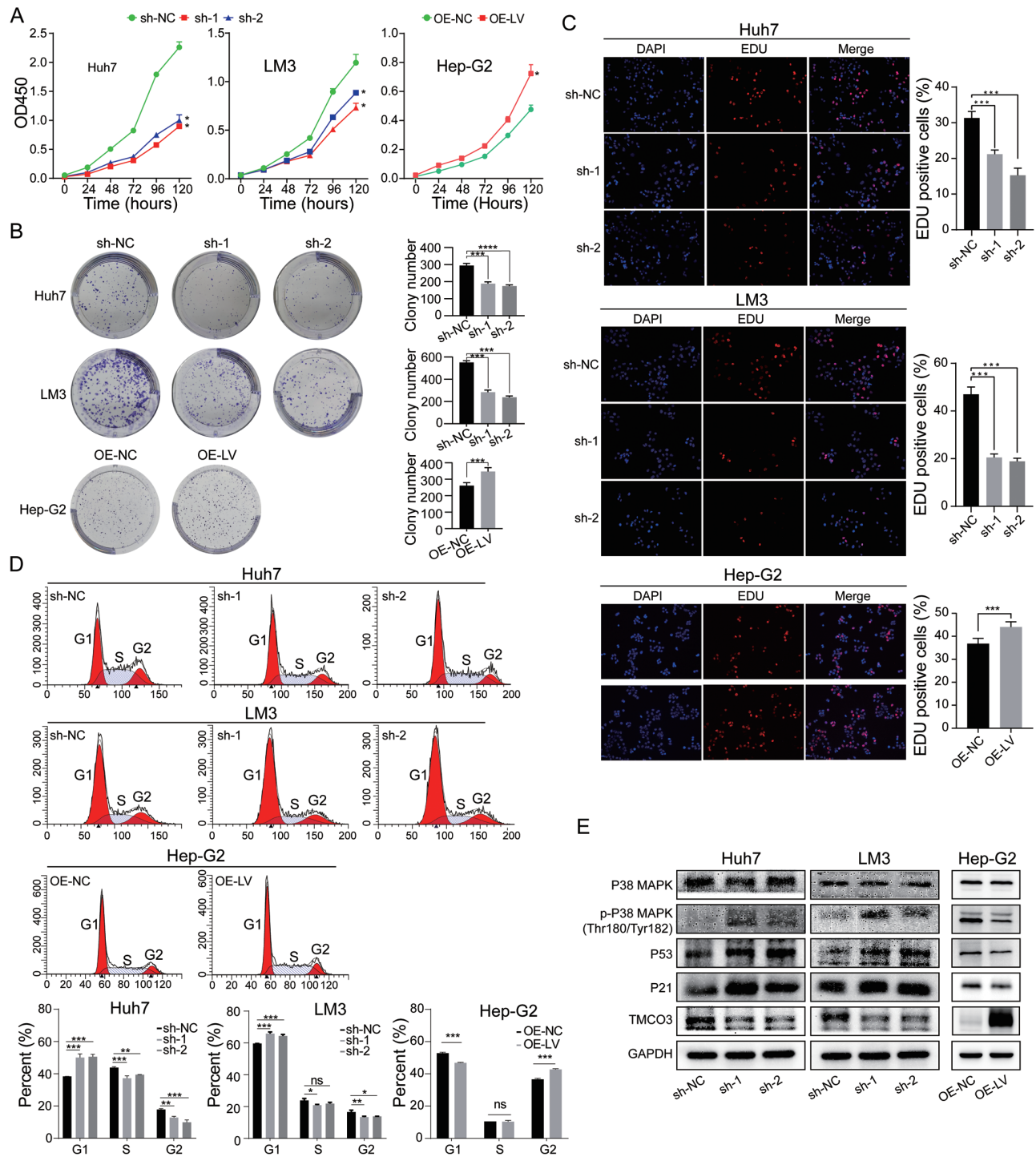
Fig. 5. Dysregulated TMCO3 affects the proliferation of HCC cells. (A) CCK-8 assays showed altered cell proliferation rate in transfected HCC cells with TMCO3 knockdown and overexpression. (B) Differential colonies formed in HCC cells with TMCO3 knockdown and overexpression. (C) Altered proportion of EDU-positive cells in HCC cells with TMCO3 knockdown and overexpression. (D) TMCO3 affected the cell cycle progression in HCC cells. (E) Western blot analyses of the protein levels of p53, p21, p38 MAPK, and phosphorylated p38 MAPK in HCC cells with the indicated treatments. ns, not significant; *$p<0.05$; **$p<0.01$; ***$p<0.001$. HCC, hepatocellular carcinoma; CCK-8, Cell Counting Kit-8; EDU, 5-Ethynyl-2'-deoxyuridine.

showed that p53 and PUMA, the apoptosis-related regulators, were upregulated in HCC cells with TMCO3 suppression, as was cleaved Bim, PARP, and Caspase 3 (Fig. 7B). When TMCO3 was overexpressed, the expression levels of the apoptotic proteins were relatively reduced in sorafenib-treated HCC cells (Fig. 7B). This finding indicates that TMCO3 might regulate the drug sensitivity of sorafenib in HCC by mediating apoptosis.
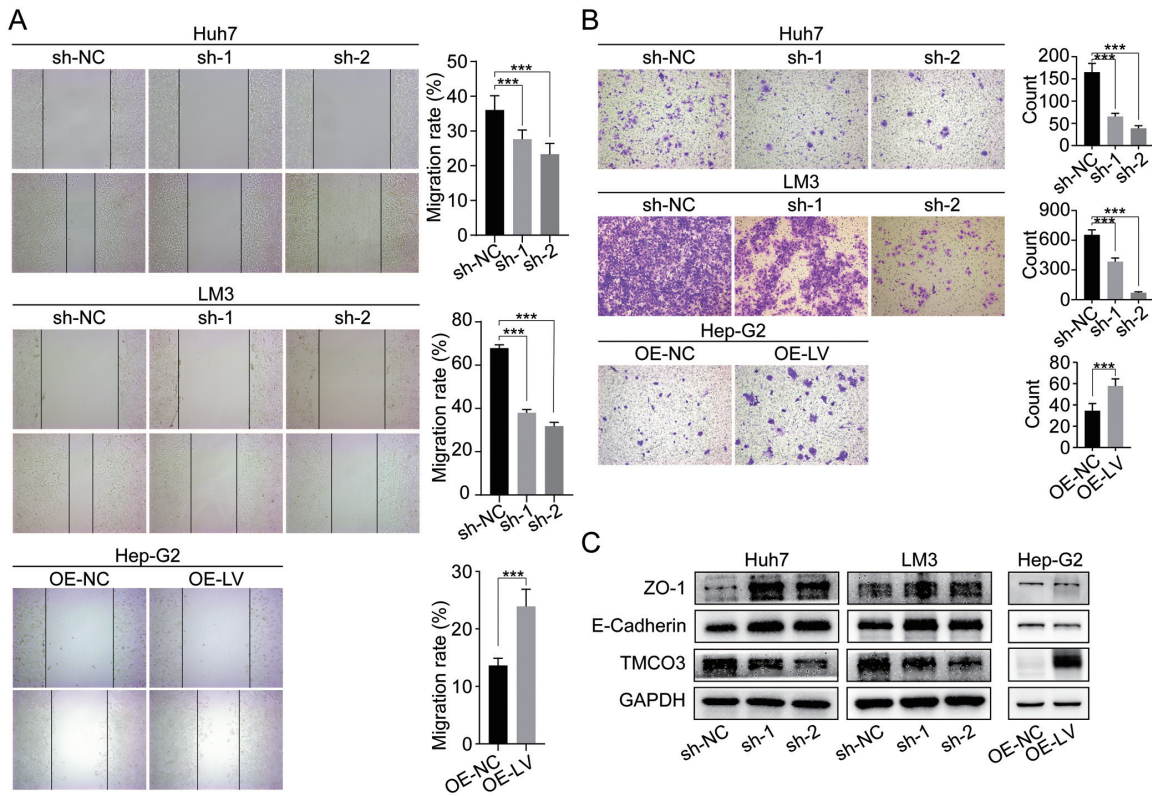
Fig. 6. Dysregulated TMCO3 mediates the migration and invasion abilities of HCC cells. (A) Scratch wound healing for cell migration abilities in transfected HCC cells with TMCO3 knockdown and overexpression. (B) Transwell Matrigel invasion assay for cell invasion abilities of transfected cells with TMCO3 knockdown and overexpression. (C) Western blot analyses of the protein levels of ZO-1 and E-cadherin in HCC cells. ***$p<0.001$. HCC, hepatocellular carcinoma.
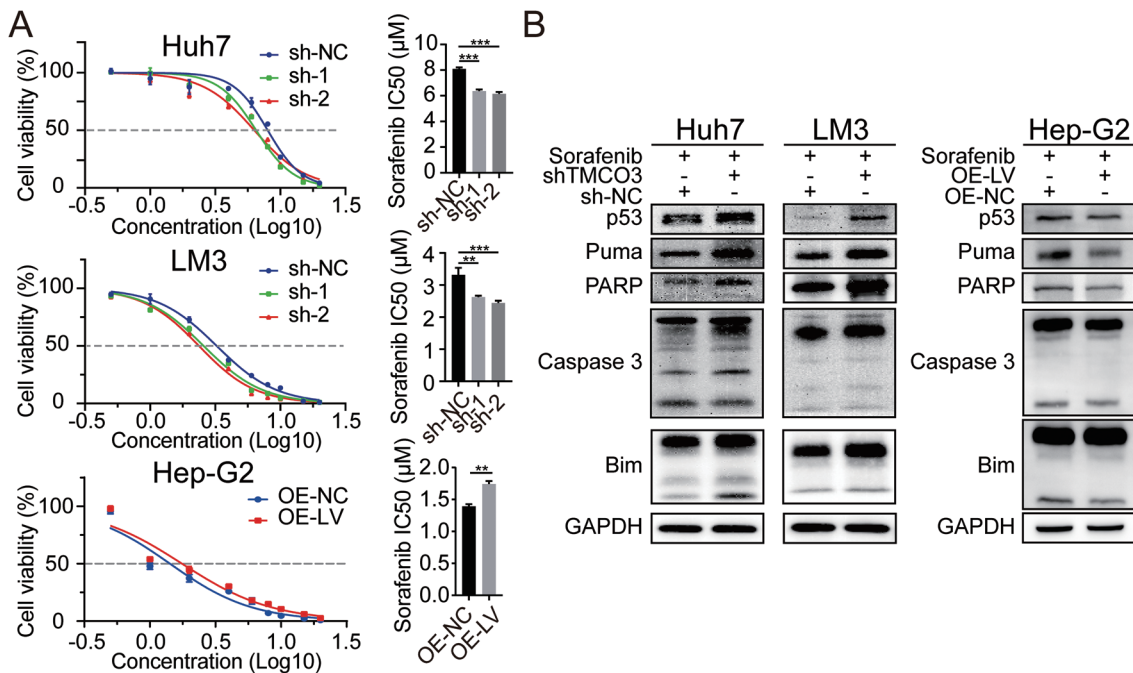

Fig. 7. TMCO3 mediates the sensitivity of HCC cells to sorafenib. (A) Sensitivity curves of HCC cells with TMCO3 knockdown and overexpression to sorafenib (0.5–20 μM). (B) Western blot analyses of the protein levels of apoptosis-related proteins in transfected HCC cells with sorafenib treatment. **$p<0.01$; ***$p<0.001$. HCC, hepatocellular carcinoma.
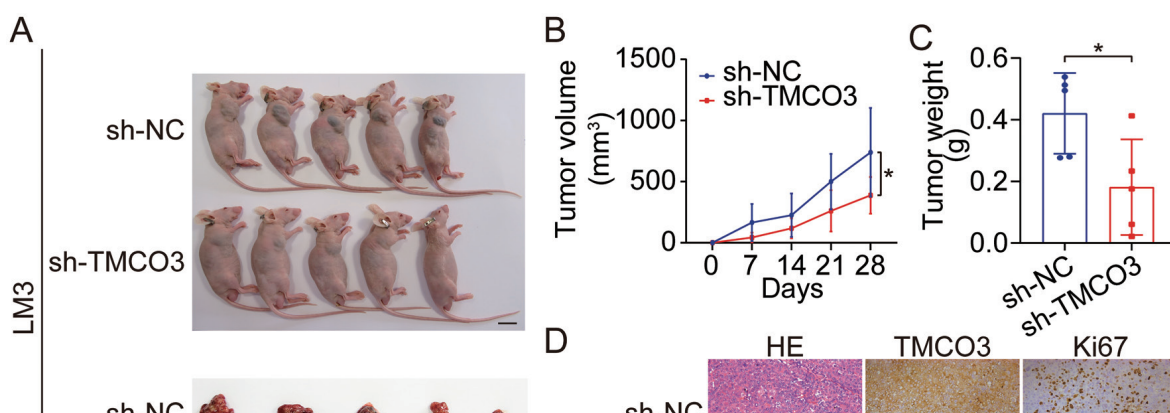
Fig. 8. Suppression of TMCO3 inhibits tumorigenicity of HCC *in vivo*. (A) Xenograft tumors developed by implanting transfected LM3 cells in nude mice. (B) Tumor volume of xenograft tumors in mice with different transplanted HCC cells. (C) Tumor weight of dissected tumors from sacrificed mice after 4 weeks. (D) Histological characteristics of xenograft tumor with hematoxylin-eosin and immunohistochemistry for TMCO3 and Ki67 expression. *p<0.05. HCC, hepatocellular carcinoma.

Suppression of TMCO3 inhibiting the HCC tumorigenicity in vivo

To explore the effect of TMCO3 on HCC tumorigenicity *in vivo*, stably transfected LM3 cells with shTMCO3 lentivirus and NC were subcutaneously implanted in the back of athymic nude mice to construct the xenograft model (Fig. 8A). When TMCO3 was knocked down in HCC-LM3 cells, the tumor growth capacity significantly decreased (tumor volume, *p*<0.05; Fig. 8B). In addition, the xenograft tumors developed from LM3 cells with TMCO3 suppression had a lower net weight (*p*<0.05; Fig. 8C). Moreover, xenograft tumors with suppressed TMCO3 expression showed a considerable decrease in positive Ki-67 staining (Fig. 8D), which further indicated a reduced proliferation rate.

Discussion

As one of the most common malignancies, studies on the pathogenesis of HCC will provide potential targets for the treatment of HCC and improve the current treatments.[15] In the present study, the oncogenic role of TMCO3 in HCC was identified using bioinformatic analyses and *in vitro* and *in vivo* experiments. The expression profile of TMCO3 in HCC was initially evaluated using transcriptome data from TCGA and validated using multiple independent datasets from GEO. All results were consistent and indicated an elevated expression of TMCO3 in HCC. The upregulated RNA and protein expression levels in HCC were further validated in another cohort from our institution by qRT-PCR, western blotting, and IHC. The prognostic significance of TMCO3 was also identified in the TCGA and our cohorts. Patients with high TMCO3 expression levels had worse OS and RFS rates. These results indicate that TMCO3 could act as a prognostic biomarker of HCC. Except for HCC, TMCO3 was also found to be significantly upregulated in CHOL, but not in other types of gastrointestinal cancer. This finding suggests that TMCO3 has a unique role in the development of hepatobiliary tumors.

Based on the above findings, we explored the functions and potential mechanisms of TMCO3 by regulating its expression in HCC cells. When TMCO3 was knocked down, cell proliferation was inhibited, and the cell cycle was arrested with an increased proportion of cells in G1 phase. Meanwhile, the protein expression levels of p53 and p21 were also increased. p53 is a transcription factor that acts as a tumor suppressor, which has been proposed to have multiple functions, such as cell cycle arrest, DNA damage repair, various pathways of cell death and metabolic alterations.[16] p21 may be expressed through the activation of p53 and is involved in the regulation of cell cycle arrest.[17,18] Hence, the G1 cell cycle arrest induced by TMCO3 suppression might be regulated through the p53/p21 axis. In addition, the suppression of TMCO3 also reduced the migration and metastasis of HCC cells, in which the inhibition of EMT might play a role. Therefore, TMCO3 may be a promising target for inhibiting HCC.

Notably, a significant correlation between TMCO3 expression and sorafenib sensitivity to HCC was identified by bioinformatic analysis and subsequently verified by functional experiments *in vitro*. When TMCO3 was silenced in hepatoma cells, the IC50 of sorafenib decreased, indicating increased sensitivity. Hence, the upregulation of TMCO3 in HCC might be involved in the development of sorafenib resistance. Sorafenib, a multiple-target tyrosine kinase inhibitor, is the first systemic therapy approved for use in the treatment of advanced HCC.[15] Its efficacy and safety have been demonstrated by multiple significant clinical trials, making it a cornerstone treatment in HCC.[3,19] However, previous studies revealed that sorafenib is only effective in 30% of HCC patients, and these patients also have a high incidence of drug resistance, which leads to the limited benefits of sorafenib.[20] Hence, the underlying mechanism involved in the development of drug resistance must be investigated. At present, multiple mechanisms have been reported to promote sorafenib resistance, such as activation of EGFR, c-Jun, and/or AKT pathway, hypoxia, EMT, promotion of cancer stem cells, tolerance to apoptosis, cell cycle dysregulation, autophagy, ferroptosis, and epigenetics (noncoding RNAs and methylation).[20,21] In the present study, we found that when TMCO3 was knocked down in HCC cells, the apoptosis induced by sorafenib was further enhanced. Hence, overexpression of TMCO3 in HCC might play a role in regulating sorafenib sensitivity by promoting apoptosis resistance. Furthermore, bioinformatic analyses revealed that the sensitivity of HCC to many other chemotherapeutic drugs is also related to the expression of TMCO3, which warrants further investigation.

Immunotherapy with immune checkpoint inhibitors has recently opened up a new era in HCC treatment.[5] Immuno-

suppressive microenvironment is an important factor leading to tumor progression and metastasis, in which immune checkpoints, such as PD-1, PD-L1, CTLA4, TIGIT, and lymphocyte activating 3 (commonly referred to as LAG3), are the key regulators.[22] Exploring the factors that influence the tumor immune microenvironment will help in the determination of new therapeutic targets or improvement of the efficacy of immunotherapy.[23] Here, we found that the overexpression of TMCO3 in HCC was positively correlated with the infiltration levels of various immune cells, including CD4^{+} T cells, macrophages, and neutrophils (all coefficients >0.4). The infiltration of these immune cells mainly provides an immunosuppressive microenvironment for tumor progression. Moreover, the expression of most immune checkpoint genes (PD-1, PD-L1, TIM3, and TIGIT) was positively correlated with TMCO3 (all coefficients >0.2). In particular, CD276 (B7-H3), another promising immunotherapy target, was significantly correlated with TMCO3 (coefficient of 0.518). Therefore, malignant phenotypes mediated by the TMCO3 may be induced by regulation of the tumor immune microenvironment, and TMCO3 could be a potential therapeutic target for HCC.

In summary, this study was the first to characterize the expression profile, potential function and prognostic significance of TMCO3 in HCC using bioinformatics analysis and *in vitro* and *in vivo* experiments. TMCO3 has been identified as an oncogenic factor, due to its involvement in the regulation of cell proliferation and metastasis. Notably, dysregulated TMCO3 may affect the sorafenib sensitivity of HCC by regulating cell apoptosis. These findings suggest that TMCO3 may be a potential target for HCC treatment.

Acknowledgments

Funding

Conflict of interest

The authors have no conflicts of interest related to this publication.

Author contributions

Study concept and design (TD, GW), acquisition of data (TD, LY, MD), analysis and interpretation of data (TD, GL, RL, HY), drafting of the manuscript (TD), critical revision of the manuscript for important intellectual content (WL, YY, GW), administrative, technical, or material support, study supervision (GW).

Data sharing statement

The datasets presented in this study can be found in online repositories (TCGA, https://portal.gdc.cancer.gov/; and GEO, https://www.ncbi.nlm.nih.gov/geo/). Other data that support the findings of this study are available within the article and supplementary files.

References

[1] Llovet JM, Kelley RK, Villanueva A, Singal AG, Pikarsky E, Roayaie S, *et al*. Hepatocellular carcinoma. Nat Rev Dis Primers 2021;7(1):6. doi:10.1038/s41572-020-00240-3, PMID:33479224.
[2] Vibert E, Schwartz M, Olthoff KM. Advances in resection and transplantation for hepatocellular carcinoma. J Hepatol 2020;72(2):262–276. doi:10.1016/j.jhep.2019.11.017, PMID:31954491.
[3] Huang A, Yang XR, Chung WY, Dennison AR, Zhou J. Targeted therapy for hepatocellular carcinoma. Signal Transduct Target Ther 2020;5(1):146. doi:10.1038/s41392-020-00264-x, PMID:32782275.
[4] SangSangro B, Sarobe P, Hervás-Stubbs S, Melero I. Advances in immunotherapy for hepatocellular carcinoma. Nat Rev Gastroenterol Hepatol 2021;18(8):525–543. doi:10.1038/s41575-021-00438-0, PMID:33850328.
[5] Pinter M, Jain RK, Duda DG. The Current Landscape of Immune Checkpoint Blockade in Hepatocellular Carcinoma: A Review. JAMA Oncol 2021;7(1):113–123. doi:10.1001/jamaoncol.2020.3381, PMID:33090190.
[6] Saier MH, Reddy VS, Moreno-Hagelsieb G, Hendargo KJ, Zhang Y, Iddamsetty V, *et al*. The Transporter Classification Database (TCDB): 2021 update. Nucleic Acids Res 2021;49(D1):D461–D467. doi:10.1093/nar/gkaa1004, PMID:33170213.
[7] Chen P, Hao X, Li W, Zhao X, Huang Y. Mutations in the TMCO3 Gene are Associated with Cornea Guttata and Anterior Polar Cataract. Sci Rep 2016;6:31021. doi:10.1038/srep31021, PMID:27484837.
[8] Duan C, Wang H, Chen Y, Chu P, Xing T, Gao C, *et al*. Whole exome sequencing reveals novel somatic alterations in neuroblastoma patients with chemotherapy. Cancer Cell Int 2018;18:21. doi:10.1186/s12935-018-0521-3, PMID:29467591.
[9] Moscovich M, LeDoux MS, Xiao J, Rampon GL, Vemula SR, Rodriguez RL, *et al*. Dystonia, facial dysmorphism, intellectual disability and breast cancer associated with a chromosome 13q34 duplication and overexpression of TFDP1: case report. BMC Med Genet 2013;14:70. doi:10.1186/1471-2350-14-70, PMID:23849371.
[10] Tang Z, Li C, Kang B, Gao G, Li C, Zhang Z. GEPIA: a web server for cancer and normal gene expression profiling and interactive analyses. Nucleic Acids Res 2017;45(W1):W98–W102. doi:10.1093/nar/gkx247, PMID:28407145.
[11] Szklarczyk D, Gable AL, Lyon D, Junge A, Wyder S, Huerta-Cepas J, *et al*. STRING v11: protein-protein association networks with increased coverage, supporting functional discovery in genome-wide experimental datasets. Nucleic Acids Res 2019;47(D1):D607–D613. doi:10.1093/nar/gky1131, PMID:30476243.
[12] Warde-Farley D, Donaldson SL, Comes O, Zuberi K, Badrawi R, Chao P, *et al*. The GeneMANIA prediction server: biological network integration for gene prioritization and predicting gene function. Nucleic Acids Res 2010;38(Suppl 2):W214–W220. doi:10.1093/nar/gkq537, PMID:20576703.
[13] Geeleher P, Cox N, Huang RS. pRRophetic: an R package for prediction of clinical chemotherapeutic response from tumor gene expression levels. PLoS One 2014;9(9):e107468. doi:10.1371/journal.pone.0107468, PMID:25229481.
[14] Li T, Fan J, Wang B, Traugh N, Chen Q, Liu JS, *et al*. TIMER: A Web Server for Comprehensive Analysis of Tumor-Infiltrating Immune Cells. Cancer Res 2017;77(21):e108–e110. doi:10.1158/0008-5472.CAN-17-0307, PMID:29092952.
[15] Llovet JM, Montal R, Sia D, Finn RS. Molecular therapies and precision medicine for hepatocellular carcinoma. Nat Rev Clin Oncol 2018;15(10):599–616. doi:10.1038/s41571-018-0073-4, PMID:30061739.
[16] Hafner A, Bulyk ML, Jambhekar A, Lahav G. The multiple mechanisms that regulate p53 activity and cell fate. Nat Rev Mol Cell Biol 2019;20(4):199–210. doi:10.1038/s41580-019-0110-x, PMID:30824861.
[17] Georgakilas AG, Martin OA, Bonner WM. p21: A Two-Faced Genome Guardian. Trends Mol Med 2017;23(4):310–319. doi:10.1016/j.molmed.2017.02.001, PMID:28279624.
[18] Engeland K. Cell cycle arrest through indirect transcriptional repression by p53: I have a DREAM. Cell Death Differ 2018;25(1):114–132. doi:10.1038/cdd.2017.172, PMID:29125603.
[19] Llovet JM, Ricci S, Mazzaferro V, Hilgard P, Gane E, Blanc JF, *et al*. Sorafenib in advanced hepatocellular carcinoma. N Engl J Med 2008;359(4):378–390. doi:10.1056/NEJMoa0708857, PMID:18650514.
[20] Tang W, Chen Z, Zhang W, Cheng Y, Zhang B, Wu F, *et al*. The mechanisms of sorafenib resistance in hepatocellular carcinoma: theoretical basis and therapeutic aspects. Signal Transduct Target Ther 2020;5(1):87. doi:10.1038/s41392-020-0187-x, PMID:32532960.
[21] Wei L, Wang X, Lv L, Liu J, Xing H, Song Y, *et al*. The emerging role of microRNAs and long noncoding RNAs in drug resistance of hepatocellular carcinoma. Mol Cancer 2019;18(1):147. doi:10.1186/s12943-019-1086-z, PMID:31651347.
[22] Sharma P, Allison JP. Dissecting the mechanisms of immune checkpoint therapy. Nat Rev Immunol 2020;20(2):75–76. doi:10.1038/s41577-020-0275-8, PMID:31925406.
[23] Feng GS, Hanley KL, Liang Y, Lin X. Improving the Efficacy of Liver Cancer Immunotherapy: The Power of Combined Preclinical and Clinical Studies. Hepatology 2021;73(Suppl 1):104–114. doi:10.1002/hep.31479, PMID:32715491.